International Journal of Nanomedicine

Dovepress

open access to scientific and medical research

Open Access Full Text Article

ORIGINAL RESEARCH

Effects of pH-sensitive chain length on release of doxorubicin from mPEG-b-PH-b-PLLA nanoparticles

This article was published in the following Dove Press journal:
International Journal of Nanomedicine
13 August 2012
Number of times this article has been viewed

Rong Liu[1,2]
Bin He[1]
Dong Li[1]
Yusi Lai[1]
Jing Chang[1]
James Z Tang[3]
Zhongwei Gu[1]

[1]National Engineering Research Center for Biomaterials, Sichuan University, Chengdu, [2]Dalian Institute of Chemical Physics Chinese Academy of Sciences, Dalian, China; [3]Department of Pharmacy, School of Applied Sciences, University of Wolverhampton, Wolverhampton, United Kingdom

Background: Two methoxyl poly(ethylene glycol)-poly(L-histidine)-poly(L-lactide) (mPEG-PH-PLLA) triblock copolymers with different poly(L-histidine) chain lengths were synthesized. The morphology and biocompatibility of these self-assembled nanoparticles was investigated.

Methods: Doxorubicin, an antitumor drug, was trapped in the nanoparticles to explore their drug-release behavior. The drug-loaded nanoparticles were incubated with HepG2 cells to evaluate their antitumor efficacy in vitro. The effects of poly(L-histidine) chain length on the properties, drug-release behavior, and antitumor efficiency of the nanoparticles were investigated.

Results: The nanoparticles were pH-sensitive. The mean diameters of the two types of mPEG-PH-PLLA nanoparticle were less than 200 nm when the pH values were 5.0 and 7.4. The nanoparticles were nontoxic to NIH 3T3 fibroblasts and HepG2 cells. The release of doxorubicin at pH 5.0 was much faster than that at pH 7.4. The release rate of $mPEG_{45}$-PH_{15}-$PLLA_{82}$ nanoparticles was much faster than that of $mPEG_{45}$-PH_{30}-$PLLA_{82}$ nanoparticles at pH 5.0.

Conclusion: The inhibition effect of $mPEG_{45}$-PH_{15}-$PLLA_{82}$ nanoparticles on the growth of HepG2 cells was greater than that of $mPEG_{45}$-PH_{30}-$PLLA_{82}$ nanoparticles when the concentration of encapsulated doxorubicin was less than 15 μg/mL.

Keywords: poly(ethylene glycol), poly(L-histidine), poly(L-lactide), pH sensitivity, doxorubicin, drug release, nanoparticle

Introduction

Biodegradable polymeric nanoparticle-based antitumor drug delivery systems have attracted much interest among biomaterials scientists[1–3] for their advantages of excellent biocompatibility, escaping of the reticuloendothelial system to avoid blood clearance and elimination from the body,[4–6] and passive targeting to tumor cells due to the enhanced permeation and retention effect.[7–11] However, passive drug delivery systems cannot guarantee optimal therapeutic efficacy in tumors with multidrug resistance.[12,13] Stimulus-sensitive drug carriers could trigger drug release in response to local environmental conditions, so this is a potentially promising approach for cancer chemotherapy. Stimuli such as pH,[14–17] enzymes,[18] and temperature[19–21] have been reported to regulate the release of antitumor drugs. Because the pH in solid tumor tissue is lower than that in normal tissue,[22,23] pH-sensitive drug release is competitive and favorable for chemotherapy.

Two main strategies are used to fabricate pH-sensitive drug delivery systems. One concerns pH-labile chemical bonds, such as hydrazone and acetal bonds,[14,24,25] to break

Correspondence: Zhongwei Gu
National Engineering Research Center for Biomaterials, Sichuan University, 29 Wangjiang Road, Chengdu 610064, China
Tel +86 28 8541 2923
Fax +86 28 8541 0653
Email zwgu@scu.edu.cn

Bin He
National Engineering Research Center for Biomaterials, Sichuan University, 29 Wangjiang Road, Chengde 610064, China
Tel +86 28 8541 2923
Fax +86 28 8541 0653
Email bhe@scu.edu.cn

and release drugs loaded into intracellular acidic endosomes. The other strategy is to induce physical dissociation[26–30] or interior structural change via variation in pH level.[31,32]

The pKa of the imidazole group in L-histidine is around 6.0, which means that protonation would occur when pH is about 6.0. For polymeric nanoparticles containing poly(L-histidine) segments, protonation of imidazole groups would lead to structural change in the nanoparticles, and this has been utilized to fabricate pH-sensitive nanodrug carriers.[26–31] In addition to protonation, the poly(L-histidine) segment has strong endosomolytic properties via its proton sponge effect and/or interaction with anionic phospholipids in the endosomal membrane[27,28,33] for easy delivery of drugs into cancer cells. In our previous work, methoxyl poly(ethylene glycol)-poly(L-histidine)-poly(L-lactide) (mPEG-PH-PLLA) triblock copolymer-based pH-sensitive nanoparticles were fabricated for antitumor drug delivery.[34] From the viewpoint of a polymeric nanoparticle drug delivery system, the chain length of the polymeric amphiphiles is an important factor affecting drug-release profiles. However, there has been no literature published concerning the effect of poly(L-histidine) chain length on drug-release behavior.

This paper focuses on the effects of poly(L-histidine) chain length on drug delivery properties as well as the antitumor efficacy of mPEG-PH-PLLA-based drug delivery systems. Two mPEG-PH-PLLA triblock copolymers with poly(L-histidine) segments of 15 and 30 repeated units were synthesized. Doxorubicin, an antitumor drug, was encapsulated in the self-assembled nanoparticles. The drug-loaded nanoparticles were incubated with HepG2 cells to study their antitumor efficacy in vitro. The effects of poly(L-histidine) chain length on drug-release behavior are discussed in detail.

Materials and methods

Materials

2-Mercaptoethanol and methoxyl poly(ethylene glycol) (mPEG, molecular weight 2000 g/mol) were purchased from Sigma-Aldrich (St Louis, MO) and used as received. N-hydroxysuccinimide was purchased from Suzhou Haofan Biological Technology Co, Ltd (Suzhou, China). N^{α}-CBZ-N^{im}-DNP-L-histidine was purchased from GL Biochem (Shanghai) Ltd (Shanghai, China). L-lactide was purchased from Purac (Schiedam, The Netherlands). Thionyl chloride was purchased from Sinopharm Chemical Reagent Co, Ltd (Shanghai, China). Triethylamine was purchased from Kelong Chemical Co, Ltd (Chengdu, China) and purified before use. d_6-DMSO was purchased from Sigma-Aldrich and used as received. Other chemicals were purchased from Sigma-Aldrich and used without further purification.

Synthesis of PEG-PH-PLLA triblock copolymer

N^{α}-CBZ-N^{im}-DNP-L-histidine was transformed to N-carboxyanhydride using thionyl chloride. N-carboxyanhydride was initiated by α-methoxy-ω-amino-poly(ethylene glycol) to prepare the methoxy-poly(ethylene glycol)-poly(L-histidine) diblock copolymer. Poly(L-lactide) was synthesized by ring-opening polymerization of L-lactide using stannous octoate as the catalyst and methoxyethoxyethanol as the initiator in a vacuum at 140°C for 48 hours. The monocarboxylated poly(L-lactide) was prepared by reacting poly(L-lactide) with succinic anhydride. The purified methoxy-poly(ethylene glycol)-poly(L-histidine) diblock copolymer was coupled with monocarboxylated poly(L-lactide) activated by N-hydroxysuccinimide to yield triblock copolymer. The triblock copolymer was deprotected by thiolysis with 2-mercaptoethanol to yield methoxy-poly(ethylene glycol)-poly(L-histidine)-poly(L-lactide). The detailed synthesis of mPEG-PH-PLLA triblock copolymers is shown in the supporting information. ^{1}H nuclear magnetic resonance (400 MHz, d_6-DMSO trimethylsilyl) δ = 8.22 – 6.79 (protons in imidazolyl), δ = 5.14 (–CH–), δ = 3.47 (–CH_2CH_2–), δ = 3.20 (–CH_2– in L-histidine), δ = 3.11(–CH– in L-histidine), and δ = 1.43 (–CH_3).

Preparation of nanoparticles

PEG-PH-PLLA block copolymers were dissolved in dimethyl sulfoxide and dropped into deionized water. The solution was transferred to a dialysis membrane tube (Spectra/Por molecular weight cutoff 2000) and dialyzed against deionized water for 24 hours. The outer phase was replaced with fresh deionized water every 8 hours. The product was separated and freeze-dried.

Doxorubicin-loaded nanoparticles

Doxorubicin hydrochloride was stirred with excess triethylamine in dimethyl sulfoxide overnight to obtain hydrophobic doxorubicin. The triblock copolymer (10 mg) was dissolved in 0.5 mL of dimethyl sulfoxide and mixed with doxorubicin solution (4 mg doxorubicin in 0.5 mL dimethyl sulfoxide) and stirred for 3.5 hours. The solution was dropped into 15 mL of deionized water and transferred to a dialysis membrane tube (Spectra/Por molecular weight cutoff 1000) to dialyze against deionized water at 4°C for 36 hours. The product in the dialysis tube was subsequently lyophilized.

The amount of entrapped doxorubicin was measured by ultraviolet absorbance at 485 nm. The drug loading content (%) and encapsulation efficiency (%) were calculated using the following equation:

$$\text{Drug loading content} = \frac{\text{Weight of doxorubicin in the nanoparticles}}{\text{Weight of drug loaded nanoparticle}} \times 100$$

$$\text{Encapsulation efficiency} = \frac{\text{The amount of doxorubicin in nanoparticles}}{\text{The amount of doxorubicin in feeding solution}} \times 100$$

Release profile of drug-loaded nanoparticles

Doxorubicin-loaded nanoparticles were dispersed in phosphate-buffered saline (0.5 mL, ionic strength 0.01 M) with different pH values (pH 7.4 and 5.0). The mixture was transferred in dialysis membrane tubes (Spectra/Por molecular weight cutoff 1000). The tubes were immersed in vials containing 25 mL of phosphate-buffered saline solution with different pH values. The vials were put in a shaking bed with a shaking rate of 120 rpm at 37°C. The outside medium of the tubes was replaced with fresh buffer solution at prescribed time intervals. The doxorubicin released was detected using a fluorescence detector with an excitation wavelength at 480 nm and an emission wavelength at 550 nm.[35]

Dynamic light scattering

Dynamic light scattering (Malvern Zetasizer Nano ZS, Malvern Instruments, Worcestershire, UK) was used to determine the average particle size of the nanoparticles at various pH values. The nanoparticles (0.5 mg/mL, ionic strength 0.01 M) were exposed to pH 5.0, 5.6, 6.3, 6.8, 7.4, and 7.9 at room temperature for 12 hours before measurement.

Transmission electron microscopy

Transmission electron microscopic images were obtained on a JEM-100CX device (JEOL, Tokyo, Japan). The transmission electron microscopy samples were prepared by dipping a copper grid with Formvar film into the freshly prepared nanoparticle solution. A few minutes after deposition, the aqueous solution was blotted away with a strip of filter paper and the samples were then dried overnight at room temperature. The samples were stained with phosphotungstic acid aqueous solution and dried in air.

Zeta potential

Variation in zeta potential of the nanoparticles in phosphate-buffered solution (0.5 mg/mL, ionic strength 0.01 M) at pH 5.0, 5.6, 6.3, 6.8, 7.4, and 7.9 was determined using the Malvern Zetasizer Nano ZS.

Cell culture

NIH 3T3 fibroblasts and HepG2 cells were cultured in Dulbecco's Modified Eagle's Medium supplemented with 10% fetal bovine serum, 100 IU/mL penicillin, and 100 µg/mL streptomycin at 37°C in a humid atmosphere with 5% CO_2. The cells were harvested with 0.02% ethylenediamine tetra-acetic acid and 0.025% trypsin, and then rinsed. The resulting cell suspension was used in the subsequent experiments.

Cytotoxicity evaluation of nanoparticles

The cytotoxicity of the nanoparticles was tested by MTT viability assay against NIH 3T3 fibroblasts and HepG2 cells. NIH 3T3 cells and HepG2 cells were separately seeded into 96-well plates at 5×10^3 cells per well in 100 µL of medium. After 24 hours of incubation, the culture medium was removed and replaced with 100 µL of medium containing the nanoparticles. The cells were incubated for another 24 hours, after which the culture medium was removed and the wells were rinsed with phosphate-buffered saline (pH 7.4). A 10 µL sample of a 5 mg/mL MTT solution in phosphate-buffered saline (pH 7.4) was added to each well. After the cells were incubated for an additional 4 hours, the medium containing unreacted MTT was removed carefully. The blue formazan crystals formed were dissolved in 100 µL of dimethyl sulfoxide for each well, and the absorbance was measured using a Thermo Fisher Scientific MK3 device (Waltham, MA) at a wavelength of 492 nm.

In vitro inhibition activity

HepG2 cells (5×10^3 cells/mL) were harvested and seeded in 96-well plates with 100 µL of Dulbecco's Modified Eagle's Medium for 24 hours before the tests. Doxorubicin, doxorubicin hydrochloride, and doxorubicin-loaded nanoparticles in Dulbecco's Modified Eagle's Medium were added to the 96-well plates with different doxorubicin concentrations (1–15 µg/mL) and incubated for 12, 24, and 36 hours. The culture medium was removed and the wells were rinsed with phosphate-buffered saline (pH 7.4). Phosphate-buffered saline (pH 7.4) containing 10 µL of MTT (5 mg/mL) solution was added to each well. After the cells were incubated for an additional 4 hours, the medium containing unreacted MTT was removed carefully. The resulting blue formazan crystals were dissolved in 100 µL of dimethyl sulfoxide for each well. The absorbance was

measured by a Thermo Fisher Scientific MK3 at a wavelength of 492 nm.

Confocal microscopy study

HepG2 cells were cultured in Dulbecco's Modified Eagle's Medium with 10% fetal bovine serum and 5% CO_2 at 37°C. HepG2 cells in their logarithm phase were seeded onto 35 mm diameter glass dishes at a cell density of 1×10^4/mL. After 24 hours, doxorubicin, doxorubicin hydrochloride, and the doxorubicin-loaded nanoparticles were dispersed and diluted in phosphate-buffered saline to reach a final doxorubicin concentration of 10 μg/mL. The mixture was added into glass dishes. After incubation at 37°C for 0.5 hours and 6 hours, the culture medium was removed and the dishes were rinsed with phosphate-buffered saline (pH 7.4). The cell nuclei were stained with DAPI and the culture medium was replaced with phosphate-buffered saline. The cells were observed using confocal laser scanning microscopy (Leica TCP SP5). Doxorubicin was excited at 485 nm, with emission at 595 nm.

Flow cytometry test

Cellular uptake was examined by flow cytometry (BD FACSAria™). In flow cytometry analysis, HepG2 cells (about 1×10^4/mL) were incubated in 24-well plates overnight, with four samples of doxorubicin and doxorubicin hydrochloride and two samples of doxorubicin-loaded nanoparticles added, ie, eight parallel samples for each one. After 6 hours of treatment, the cells were rinsed with phosphate-buffered saline, trypsinized, and resuspended in 500 μL of phosphate-buffered saline. Flow cytometry was used to analyze approximately 10^4 cells from each sample.

Results and discussion

Two mPEG-PH-PLLA triblock copolymers with different poly(L-histidine) chain lengths were synthesized. The repeated numbers of L-histidine in the poly(L-histidine) blocks were 15 and 30, respectively. The repeated units of the lactic acid designed were 82. The synthetic route and characterization of the mPEG-PH-PLLA triblock copolymers are presented in the supporting information (Figures S1, S2, and Table S1). The two triblock copolymers were named $mPEG_{45}$-PH_{15}-$PLLA_{82}$ and $mPEG_{45}$-PH_{30}-$PLLA_{82}$. The critical aggregation concentration of the self-assembled nanoparticles was tested by a steady-state pyrene fluorescence method reported elsewhere.[36] The calculated critical aggregation concentrations of the $mPEG_{45}$-PH_{15}-$PLLA_{82}$ and $mPEG_{45}$-PH_{30}-$PLLA_{82}$ nanoparticles were 3 μg/mL and 8 μg/mL, respectively. This suggests that the nanoparticles with a shorter poly(L-histidine) chain length were more stable due to their lower critical aggregation concentration.

The zeta potential is an important parameter for determining the surface charge on nanoparticles, which is helpful for understanding the relationship between the protonation and pH sensitivity of mPEG-PH-PLLA nanoparticles. The mean diameters and zeta potentials of two nanoparticles with different pH values are shown in Figure 1. The mean particle size of the $mPEG_{45}$-PH_{15}-$PLLA_{82}$ nanoparticles was measured with pH ranging from 5.0 to 7.9 (Figure 1A). Interestingly, the mean diameter of the nanoparticles was about 131 nm at pH 5.0 and about 1.3 μm when the pH was increased to 6.4. The mean diameter decreased dramatically from 1.3 μm to 100 nm when the pH was changed from 6.4 to 7.9. The maximal diameter of the nanoparticles appeared around the pKa of the imidazole group. Size variation in the nanoparticles was thought to be attributable to electrostatic repulsion. At pH 6.4, the charge on the nanoparticles was almost neutral and electrostatic repulsion between the nanoparticles was the weakest, so the nanoparticles aggregated together to form microsized particles. The zeta potential result is consistent with this theory. The neutral point of the $mPEG_{45}$-PH_{15}-$PLLA_{82}$ nanoparticles was about pH 6.5 (Figure 1C). When environmental pH was lower or higher than 6.5, the poly(L-histidine) blocks were positively or negatively charged. The zeta potential of the nanoparticles was in the range of 0–12 mV when pH varied from 6.5 to 5.0. The zeta potential of the nanoparticles was negative, reaching −12 mV, when pH was increased from 6.5 to 7.9. Both the highest positive and negative zeta potentials for the nanoparticles corresponded to the smallest particle sizes because of electrostatic repulsion between the charged nanoparticles. Changes in mean diameter and zeta potential of the $mPEG_{45}$-PH_{30}-$PLLA_{82}$ nanoparticles were similar to those of the $mPEG_{45}$-PH_{15}-$PLLA_{82}$ nanoparticles when pH was increased from 5.0 to 7.9.

The morphology of nanoparticles with different pH values was observed by transmission electron microscopy (Figure 2). The size of the $mPEG_{45}$-PH_{15}-$PLLA_{82}$ nanoparticles (Figure 2A and B) was about 130–140 nm at pH 5.0 and about 100–110 nm at pH 7.4, while that of the $mPEG_{45}$-PH_{30}-$PLLA_{82}$ nanoparticles was about 70–80 nm at pH 5.0 and about 170–180 nm at pH 7.4 (Figure 2C and D). Particle size in the transmission electron micrographs was consistent with the results of dynamic light scattering, as shown in Figure 1.

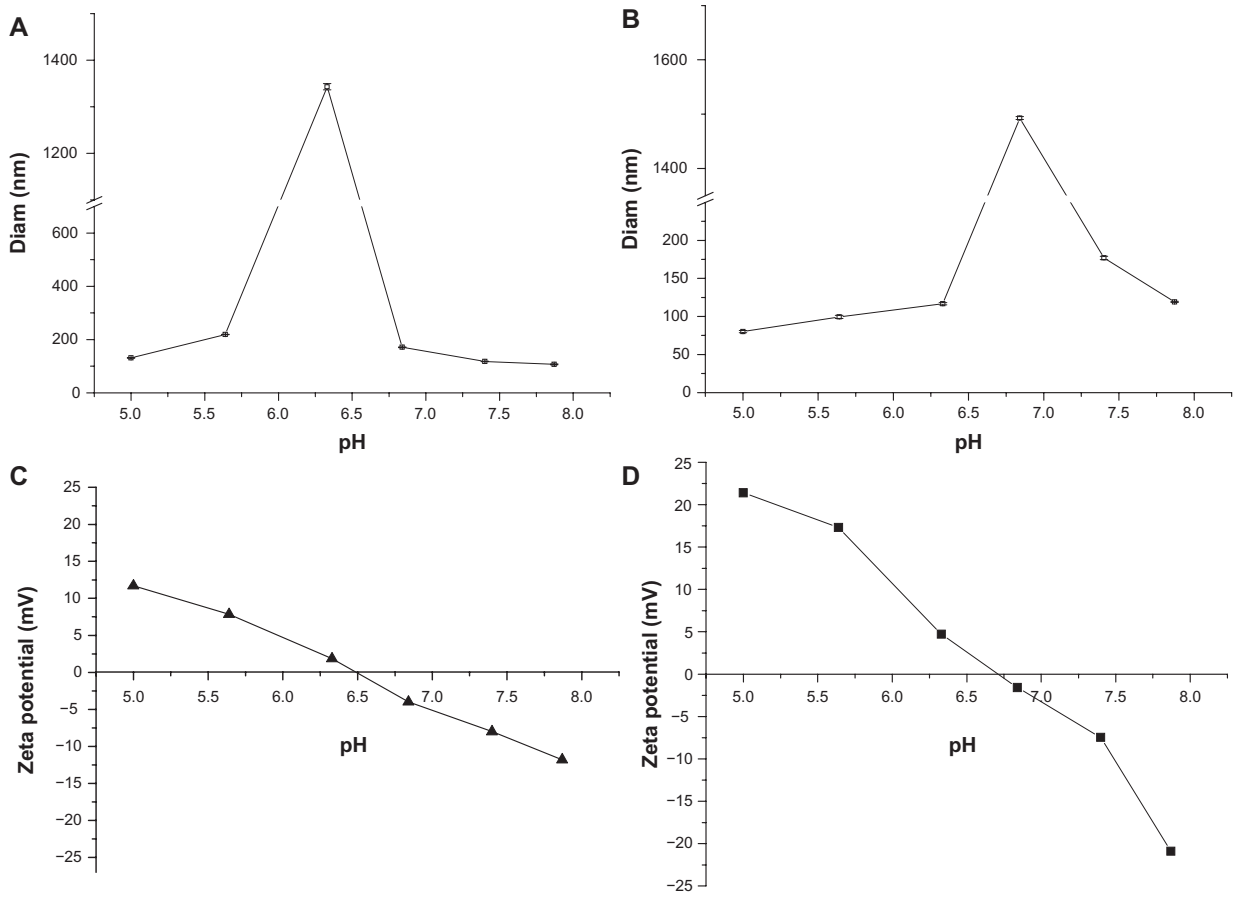

Figure 1 Mean diameters of nanoparticles of $mPEG_{45}$-PH_{15}-$PLLA_{82}$ (**A**) and $mPEG_{45}$-PH_{30}-$PLLA_{82}$ (**B**), and zeta potential of $mPEG_{45}$-PH_{15}-$PLLA_{82}$ (**C**) and $mPEG_{45}$-PH_{30}-$PLLA_{82}$ (**D**) nanoparticles at different pH values.
Abbreviation: mPEG-PH-PLLA, methoxyl poly(ethylene glycol)-poly(L-histidine)-poly(L-lactide).

The drug-loading content and encapsulation efficiency of the nanoparticles are presented as supporting information in Table S1. The release profile of the doxorubicin-loaded nanoparticles is presented in Figure 3. Doxorubicin and doxorubicin hydrochloride were used as controls. As shown in Figure 3, hydrophilic doxorubicin hydrochloride was released very rapidly. The accumulated release reached nearly 100% within 2 hours. The release rate of doxorubicin was very slow because of its hydrophobicity. The accumulated release rate was less than 10% within 76 hours. Doxorubicin release from the nanoparticles at pH 5.0 was much faster than that at pH 7.4. After 24 hours, accumulated release rates of both nanoparticles at pH 7.4 were less than 40%, but the release rate of $mPEG_{45}$-PH_{15}-$PLLA_{82}$ nanoparticles was nearly 80% and that of $mPEG_{45}$-PH_{30}-$PLLA_{82}$ nanoparticles was 55% at pH 5.0. When the release time was extended to 76 hours, the accumulated release of doxorubicin-loaded $mPEG_{45}$-PH_{30}-$PLLA_{82}$ nanoparticles reached 80%. A possible reason was that, at pH 5.0, the poly(L-histidine) blocks in both nanoparticles were protonated and swelled, and for the longer poly(L-histidine) chain in the $mPEG_{45}$-PH_{30}-$PLLA_{82}$ nanoparticles, interactions such as hydrogen bonding within the poly(L-histidine) segments were stronger than in $mPEG_{45}$-PH_{15}-$PLLA_{82}$ nanoparticles, which retarded the release of doxorubicin. Therefore, the release rate from doxorubicin-loaded $mPEG_{45}$-PH_{30}-$PLLA_{82}$ nanoparticles was slower than that from doxorubicin-loaded $mPEG_{45}$-PH_{15}-$PLLA_{82}$ nanoparticles. At pH 7.4, the poly(L-histidine) segments were not protonated and the poly(L-histidine) layer was compact, so the release of doxorubicin from the two nanoparticles was comparable.

The cytotoxicity evaluation of the two nanoparticles was tested using NIH 3T3 fibroblasts (Figure 4) and HepG2 liver cancer cells (Figure 5). The MTT assay was used to test cell viability. As shown in Figures 4 and 5, cell viability with the two nanoparticles was higher than 90%, regardless of concentration. Cell viability with the $mPEG_{45}$-PH_{15}-$PLLA_{82}$ nanoparticles was higher than that with the $mPEG_{45}$-PH_{30}-$PLLA_{82}$ nanoparticles. Interestingly, when the concentration

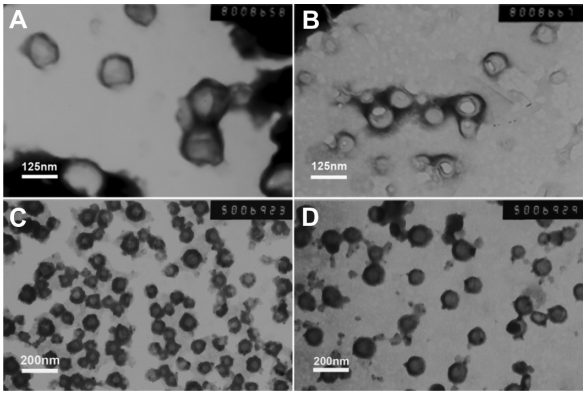

Figure 2 Transmission electron microscopic images of nanoparticles at different pH levels. (**A**) and (**B**) are $mPEG_{45}$-PH_{15}-$PLLA_{82}$ nanoparticles. (**C**) and (**D**) are $mPEG_{45}$-PH_{30}-$PLLA_{82}$ nanoparticles. The pH value of (**A**) and (**C**) was 5.0 and that of (**B**) and (**D**) was 7.4.
Abbreviation: mPEG-PH-PLLA, methoxyl poly(ethylene glycol)-poly(L-histidine)-poly(L-lactide).

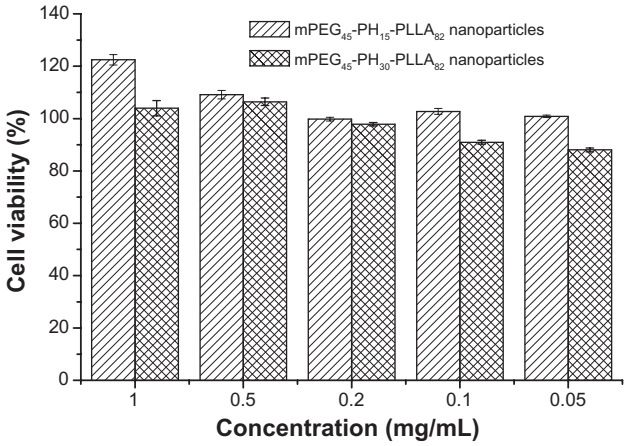

Figure 4 Cell viability of $mPEG_{45}$-PH_{15}-$PLLA_{82}$ and $mPEG_{45}$-PH_{30}-$PLLA_{82}$ nanoparticles incubated with NIH 3T3 fibroblasts for 24 hours.
Abbreviation: mPEG-PH-PLLA, methoxyl poly(ethylene glycol)-poly(L-histidine)-poly(L-lactide).

of $mPEG_{45}$-PH_{15}-$PLLA_{82}$ nanoparticles was higher than 0.5 mg/mL, it seemed that the $mPEG_{45}$-PH_{15}-$PLLA_{82}$ nanoparticles could promote proliferation of both NIH 3T3 fibroblasts and HepG2 cells. This may be attributed to the nutrient effect of the poly(L-histidine) chains. These results demonstrate that the nanoparticles were nontoxic to NIH 3T3 fibroblasts and HepG2 cells.

The cellular uptake of doxorubicin-loaded nanoparticles was studied using confocal laser scanning microscopy. Figure 6 shows the confocal microscopy photographs of HepG2 cells incubated with doxorubicin hydrochloride, doxorubicin, and the two doxorubicin-loaded nanoparticles for 0.5 and 6 hours. In the first half hour, doxorubicin hydrochloride was mainly distributed in the nucleus of HepG2 cells. Moreover, the intensity of red fluorescence for free doxorubicin hydrochloride in the nucleus was stronger than that in the cytoplasm. For the doxorubicin-loaded nanoparticles and doxorubicin alone, red fluorescence was only observed in the cytoplasm, and the intensity of red fluorescence in all three samples was weak.

In photographs taken after 6 hours of cultivation, the red fluorescence of doxorubicin hydrochloride, doxorubicin, and doxorubicin-loaded nanoparticles could be observed, not only in the cytoplasm but also in the nuclei. However, in the cytoplasm, the red fluorescence of doxorubicin hydrochloride was the strongest, and that of doxorubicin was the weakest. The red fluorescence of doxorubicin-loaded $mPEG_{45}$-PH_{15}-$PLLA_{82}$ nanoparticles

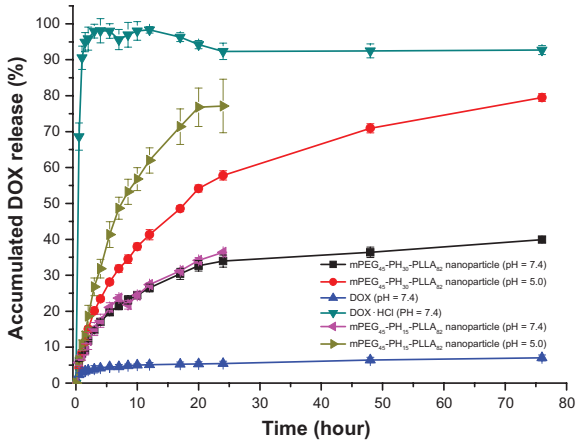

Figure 3 Release profiles of doxorubicin-loaded $mPEG_{45}$-PH_{15}-$PLLA_{82}$ and $mPEG_{45}$-PH_{30}-$PLLA_{82}$ nanoparticles at different pH values.
Abbreviations: DOX, doxorubicin; mPEG-PH-PLLA, methoxyl poly(ethylene glycol)-poly(L-histidine)-poly(L-lactide).

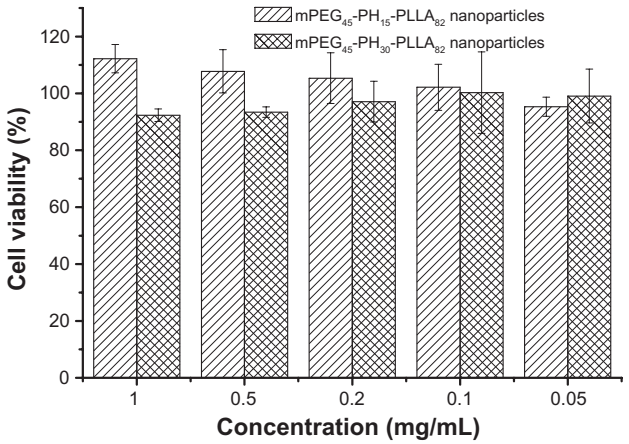

Figure 5 Cell viability of $mPEG_{45}$-PH_{15}-$PLLA_{82}$ and $mPEG_{45}$-PH_{30}-$PLLA_{82}$ nanoparticles incubated with HepG2 cells for 24 hours.
Abbreviation: mPEG-PH-PLLA, methoxyl poly(ethylene glycol)-poly(L-histidine)-poly(L-lactide).

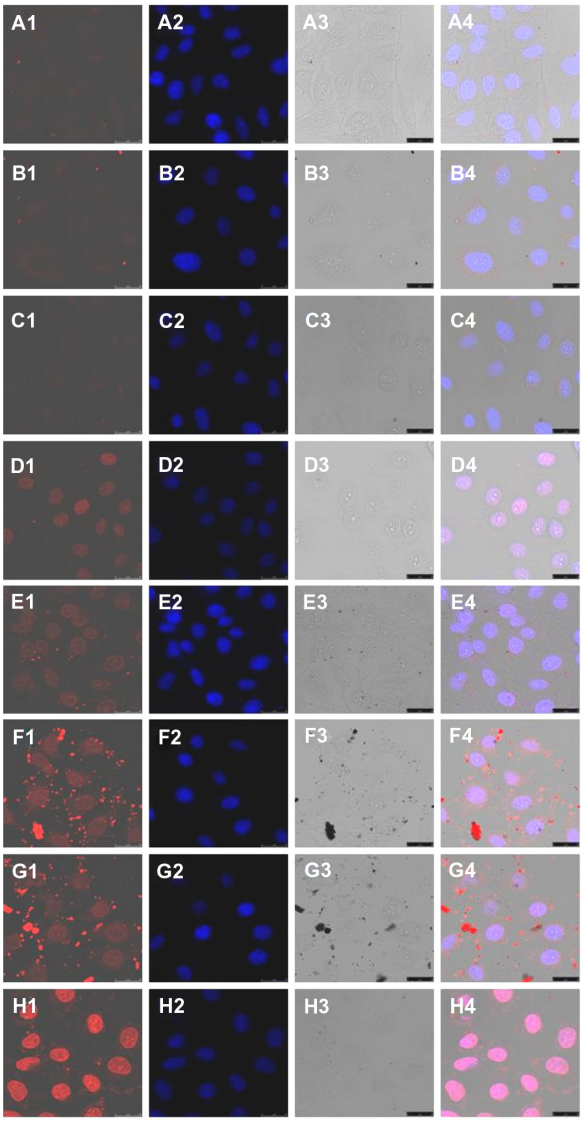

Figure 6 Confocal microscopy photographs of HepG2 cells incubated with doxorubicin-loaded nanoparticles. (**A1–A4**) doxorubicin for 0.5 hours; (**B1–B4**) doxorubicin-loaded $mPEG_{45}$-PH_{15}-$PLLA_{82}$ nanoparticles for 0.5 hours; (**C1–C4**) doxorubicin-loaded $mPEG_{45}$-PH_{30}-$PLLA_{82}$ nanoparticles for 0.5 hours; (**D1–D4**) doxorubicin hydrochloride for 0.5 hours; (**E1–E4**) doxorubicin for 6 hours; (**F1–F4**) doxorubicin-loaded $mPEG_{45}$-PH_{15}-$PLLA_{82}$ nanoparticles for 6 hours; (**G1–G4**) doxorubicin-loaded $mPEG_{45}$-PH_{30}-$PLLA_{82}$ nanoparticles for 6 hours; (**H1–H4**) doxorubicin hydrochloride for 6 hours. Note: The four photographs from left to right are red doxorubicin, stained nucleus, bright field, and overlapped graphs.
Abbreviation: mPEG-PH-PLLA, methoxyl poly(ethylene glycol)-poly(L-histidine)-poly(L-lactide).

was comparable with that of doxorubicin-loaded $mPEG_{45}$-PH_{30}-$PLLA_{82}$ nanoparticles. Being a hydrophilic drug, doxorubicin hydrochloride was easily internalized in HepG2 cells and diffused into the nuclei. Doxorubicin was hydrophobic, so was poorly internalized in cells by diffusion. The drug-loaded nanoparticles were endocytosed to deliver doxorubicin into the cytoplasm, and the trapped drug was released from acidic endosomes and diffused into the nuclei.

Flow cytometry analysis was carried out to evaluate endocytosis of doxorubicin hydrochloride, doxorubicin, and two doxorubicin-loaded nanoparticles quantitatively (the doxorubicin concentration was 10 μg/mL). Fluorescence intensity was proportional to the amount of doxorubicin internalized in HepG2 cells. The flow cytometry results are shown in Figure 7. When HepG2 cells were incubated with doxorubicin hydrochloride, doxorubicin, and doxorubicin-loaded nanoparticles for 6 hours, the fluorescence intensity of doxorubicin hydrochloride was the highest in the four samples. Furthermore, the intensity of the doxorubicin-loaded nanoparticles was higher than that of doxorubicin. This suggests that the cellular uptake of doxorubicin was improved by encapsulation. These results are in agreement with the results of confocal laser scanning microscopy and release profiles.

The morphologies of the HepG2 cells incubated with the two drug-loaded nanoparticles, doxorubicin and doxorubicin hydrochloride (doxorubicin concentration 15 μg/mL), for 36 hours are shown in Figure 8. Most of the cells attached and stretched well on the cell culture plate (Figure 8A). All the cells detached and shrank to spheres in the doxorubicin hydrochloride sample (Figure 8B). Some cells detached and some stretched well in the doxorubicin sample (Figure 8C). Most of the cells shrank to spheres in both types of nanoparticles (Figure 8D and E).

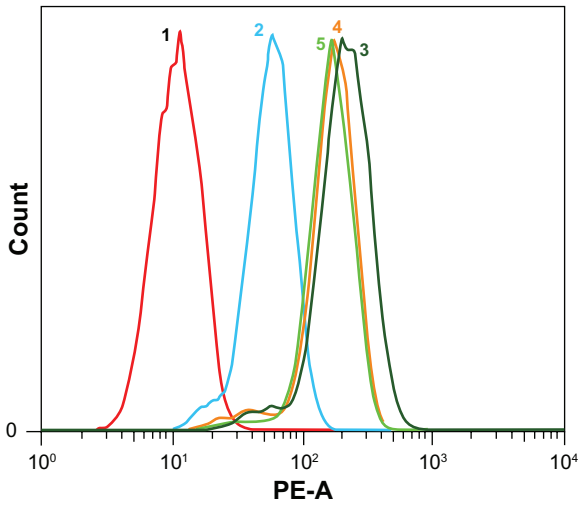

Figure 7 Flow cytometry results of doxorubicin, doxorubicin hydrochloride, and doxorubicin-loaded $mPEG_{45}$-PH_{15}-$PLLA_{82}$ and $mPEG_{45}$-PH_{30}-$PLLA_{82}$ nanoparticles incubated with HepG2 cells at 37°C for 6 hours (doxorubicin concentration 10 μg/mL).
Notes: 1, control; 2, doxorubicin; 3, doxorubicin hydrochloride; 4, doxorubicin-loaded $mPEG_{45}$-PH_{15}-$PLLA_{82}$ nanoparticles; 5, doxorubicin-loaded $mPEG_{45}$-PH_{30}-$PLLA_{82}$ nanoparticles.
Abbreviation: mPEG-PH-PLLA, methoxyl poly(ethylene glycol)-poly(L-histidine)-poly(L-lactide).

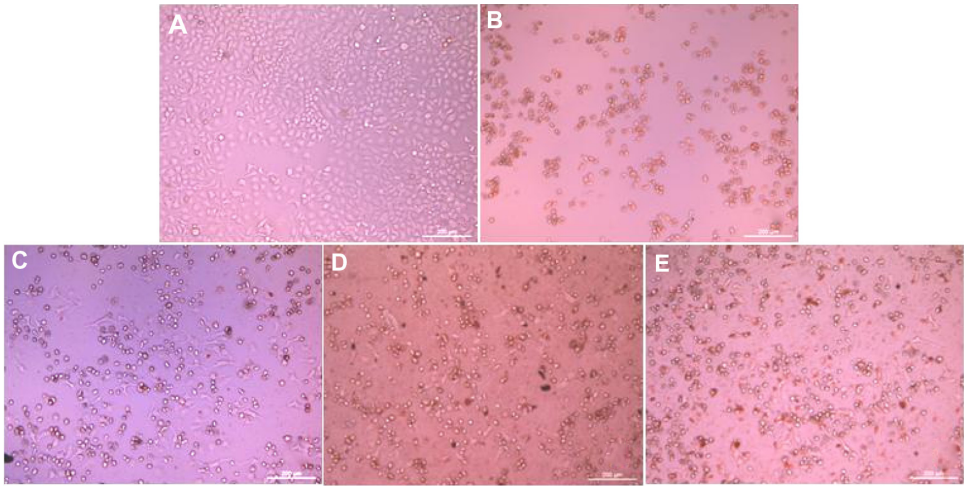

Figure 8 Morphology of HepG2 cells incubated with doxorubicin-loaded nanoparticles, the time was 36 hours and the concentration of doxorubicin was 15 μg/mL. (**A**) Cell culture plate, (**B**) doxorubicin hydrochloride, (**C**) doxorubicin, (**D**) doxorubicin-loaded $mPEG_{45}$-PH_{15}-$PLLA_{82}$ nanoparticles, and (**E**) doxorubicin-loaded $mPEG_{45}$-PH_{30}-$PLLA_{82}$ nanoparticles.
Abbreviation: mPEG-PH-PLLA, methoxyl poly(ethylene glycol)-poly(L-histidine)-poly(L-lactide).

The in vitro anticancer activity of the drug-loaded nanoparticles was investigated. The quantitative results are shown in Figures 9 and 10. In Figure 9, the drug concentration was 15 μg/mL, and the viability of HepG2 cells was measured at 12, 24, and 36 hours. The cell viability of all four samples decreased when the incubation time was increased from 12 to 36 hours. At each time point, the lowest cell viability was for doxorubicin hydrochloride and the highest was for doxorubicin. There was no significant difference in inhibition bioactivity ($P > 0.05$) for the two drug-loaded nanoparticles when the drug concentration was 15 μg/mL.

In Figure 10, the drug concentrations were 1, 5, 10, and 15 μg/mL. With increasing concentration, cell viability with doxorubicin and the drug-loaded nanoparticles decreased markedly. However, with doxorubicin hydrochloride, there was less decrease when the concentration was higher than 5 μg/mL, suggesting that 5 μg/mL was the critical effective concentration of doxorubicin hydrochloride to kill HepG2. In addition, when the drug concentration was increased from 1 to 10 μg/mL, the anticancer activity of doxorubicin-loaded $mPEG_{45}$-PH_{15}-$PLLA_{82}$ nanoparticles was higher than that of doxorubicin-loaded $mPEG_{45}$-PH_{30}-$PLLA_{82}$ nanoparticles ($P < 0.05$).

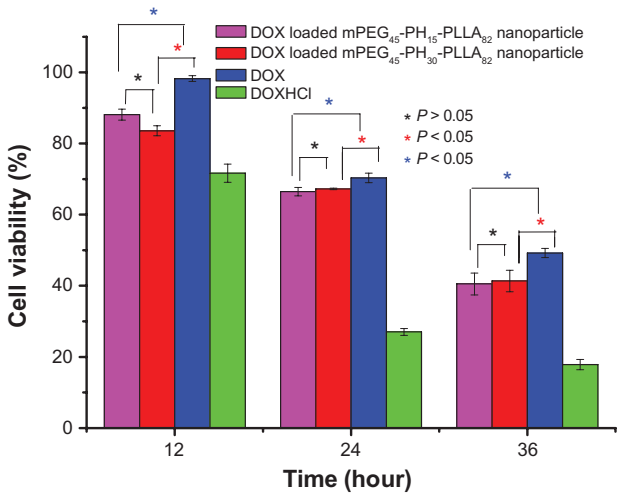

Figure 9 In vitro antitumor activity of doxorubicin-loaded nanoparticles incubated with HepG2 cells, drug concentration was 15 μg/mL.
Abbreviations: DOX, doxorubicin; mPEG-PH-PLLA, methoxyl poly(ethylene glycol)-poly(L-histidine)-poly(L-lactide).

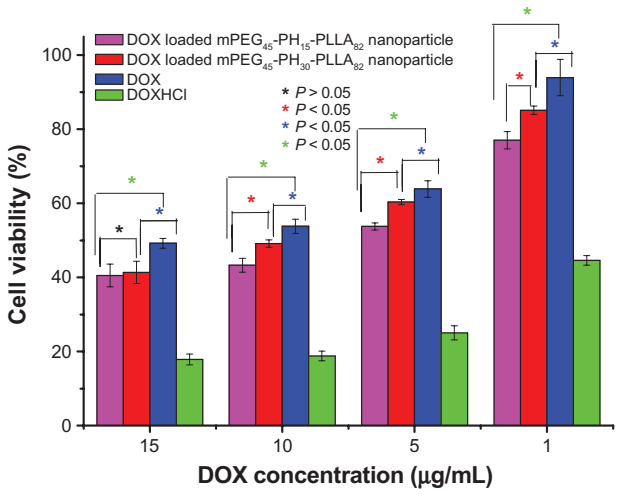

Figure 10 In vitro antitumor activity of doxorubicin-loaded nanoparticles with different drug concentrations, incubation time was 36 hours.
Abbreviations: DOX, doxorubicin; mPEG-PH-PLLA, methoxyl poly(ethylene glycol)-poly(L-histidine)-poly(L-lactide).

Conclusion

Two pH-sensitive nanoparticles of methoxyl poly(ethylene glycol)-poly(L-histidine)-poly(L-lactide) triblock copolymers with different poly(L-histidine) chain lengths were prepared. The mean diameters of the two nanoparticles were tunable from nanoscale to microscale at different pH values. The nanoparticles were nontoxic to NIH 3T3 fibroblasts and HepG2 liver cancer cells. Drug release from the loaded nanoparticles was pH-sensitive. Accumulated release of the two nanoparticles at pH 7.4 was less than 40% within 76 hours, whereas at pH 5.0, accumulated drug release of doxorubicin-loaded $mPEG_{45}$-PH_{15}-$PLLA_{82}$ nanoparticles was nearly 80%, and that of doxorubicin-loaded $mPEG_{45}$-PH_{30}-$PLLA_{82}$ nanoparticles was around 55% within 24 hours. The drug loaded nanoparticles were internalized into HepG2 cells efficiently. When the doxorubicin concentration was less than 10 μg/mL, the anticancer activity of doxorubicin-loaded $mPEG_{45}$-PH_{15}-$PLLA_{82}$ nanoparticles was better than that of doxorubicin-loaded $mPEG_{45}$-PH_{30}-$PLLA_{82}$ nanoparticles.

Acknowledgments

This research was supported by the National 973 Program (2011CB606206), National Science Foundation of China (50830105, 31170921, 51133004), Program for New Century Excellent Talents in University (NCET-10-0564), Ministry of Science and Technology (2010DFA51550), and European Commission Research and Innovation (PIRSES-GA-2011-295218).

Disclosure

The authors report no conflicts of interest in this work.

References

1. Bae Y, Jang WD, Nishiyama N, Fukushima S, Kataoka K. Multifunctional polymeric micelles with folate-mediated cancer cell targeting and pH-triggered drug releasing properties for active intracellular drug delivery. *Mol Biosyst*. 2005;1:242–250.
2. Yan H, Jiang WM, Zhang YX, et al. Novel multi-biotin grafted poly(lactic acid) and its self-assembling nanoparticles capable of binding to streptavidin. *Int J Nanomedicine*. 2012;7:457–465.
3. Karavelidis V, Karavas E, Giliopoulos D, et al. Evaluating the effects of crystallinity in new biocompatible polyester nanocarriers on drug release behavior. *Int J Nanomedicine*. 2011;6:3021–3032.
4. Kwon GS, Kataoka K. Block-copolymer micelles as long-circulating drug vehicles. *Adv Drug Deliv Rev*. 1995;16:295–309.
5. Kwon GS, Okano T. Polymeric micelles as new drug carriers. *Adv Drug Deliv Rev*. 1996;21:107–116.
6. Gu PF, Xu H, Sui BW, et al. Polymeric micelles based on poly(ethylene glycol) block poly(racemic amino acids) hybrid polypeptides: conformation-facilitated drug-loading behavior and potential application as effective anticancer drug carriers. *Int J Nanomedicine*. 2012;7:109–122.
7. Son YJ, Jang JS, Cho YW, et al. Biodistribution and anti-tumour efficacy of doxorubicin loaded glycol-chitosan nanoaggregates by EPR effect. *J Control Release*. 2003;91:135–145.
8. Kataoka K, Kwon GS, Yokoyama M, Okano T, Sakurai Y. Block-copolymer micelles as vehicles for drug delivery. *J Control Release*. 1993;24:119–132.
9. Ranganathan R, Madanmohan S, Kesavan A, et al. Nanomedicine: towards development of patient-friendly drug-delivery systems for oncological applications. *Int J Nanomedicine*. 2012;7:1043–1060.
10. Wang K, Liu L, Zhang T, et al. Oxaliplatin-incorporated micelles eliminate both cancer stem-like and bulk cell populations in colorectal cancer. *Int J Nanomedicine*. 2011;6:3207–3218.
11. Cai LL, Liu P, Li X, et al. RGD peptide-mediated chitosan-based polymeric micelles targeting delivery for integrin-overexpressing tumor cells. *Int J Nanomedicine*. 2011;6:3499–3508.
12. Larsen AK, Escargueil AE, Skladanowski A. Resistance mechanisms associated with altered intracellular distribution of anticancer agents. *Pharmacol Ther*. 2000;88:217–229.
13. Bennis S, Chapey C, Couvreur P, Robert J. Enhanced cytotoxicity of doxorubicin encapsulated in polyhexylcyanoacrylate nanospheres against multi-drug-resistant tumor cells in culture. *Eur J Cancer*. 1994;30:89–93.
14. Gillies ER, Frechet JM. pH-responsive copolymer assemblies for controlled release of doxorubicin. *Bioconjug Chem*. 2005;16:361–368.
15. Frutos G, Prior-Cabanillas A, París R, Quijada-Garrido I. A novel controlled drug delivery system based on pH-responsive hydrogels included in soft gelatin capsules. *Acta Biomater*. 2010;6:4650–4656.
16. Butsele KV, Morille M, Passirani C, et al. Stealth properties of poly(ethylene oxide)-based triblock copolymer micelles: a prerequisite for a pH-triggered targeting system. *Acta Biomater*. 2011;7:3700–3707.
17. Li P, Liu DH, Miao L, et al. A pH-sensitive multifunctional gene carrier assembled via layer-by-layer technique for efficient gene delivery. *Int J Nanomedicine*. 2012;7:925–939.
18. Putnam D, Kopecek J. Enantioselective release of 5-fluorouracil from N-(2-hydroxypropyl) methacrylamide-based copolymers via lysosomal enzymes. *Bioconjug Chem*. 1995;6:483–492.
19. Cammas S, Suzuki K, Sone C, Sakurai Y, Kataoka K, Okano T. Thermo-responsive polymer nanoparticles with a core-shell micelle structure as site-specific drug carriers. *J Control Release*. 1997;48:157–164.
20. Chung JE, Yokoyama M, Okano T. Inner core segment design for drug delivery control of thermo-responsive polymeric micelles. *J Control Release*. 2000;65:93–103.
21. Liu S, Wiradharma N, Gao S, Tong Y, Yang Y. Bio-functional micelles self-assembled from a folate-conjugated block copolymer for targeted intracellular delivery of anticancer drugs. *Biomaterials*. 2007;28:1423–1433.
22. Engin K, Leeper DB, Cater JR, Thistlethwaite AJ, Tupchong L, McFarlane JD. Extracellular pH distribution in human tumors. *Int J Hyperthermia*. 1995;11:211–216.
23. Ojugo AS, McSheehy PM, McIntyre DJ, et al. Measurement of the extracellular pH of solid tumours in mice by magnetic resonance spectroscopy: a comparison of exogenous ^{19}F and ^{31}P probes. *NMR Biomed*. 1999;12:495–504.
24. Sawant RM, Hurley JP, Salmaso S, et al. "Smart" drug delivery systems: double-targeting pH-responsive pharmaceutical nanocarriers. *Bioconjug Chem*. 2006;17:943–949.
25. Bae Y, Nishiyama N, Fukushima S, Koyama H, Yasuhiro M, Kataoka K. Preparation and biological characterization of polymeric micelle drug carriers with intracellular pH-triggered drug release property: tumor permeability, controlled subcellular drug distribution, and enhanced in vivo antitumor efficacy. *Bioconjug Chem*. 2005;16:122–130.
26. Lee ES, Shin HJ, Na K, Bae YH. Poly(L-histidine)-PEG block copolymer micelles and pH-induced destabilization. *J Control Release*. 2003;90:363–374.

27. Lee ES, Na K, Bae YH. Polymeric micelle for tumor pH and folate-mediated targeting. *J Control Release*. 2003;91:103–113.
28. Lee ES, Na K, Bae YH. Super pH-sensitive multifunctional polymeric micelle. *Nano Lett*. 2005;5:325–329.
29. Kim GM, Bae YH, Jo WH. pH-induced micelle formation of poly(histidine-co-phenylalanine)-block-poly(ethylene glycol) in aqueous media. *Macromol Biosci*. 2005;5:1118–1124.
30. Lee ES, Na K, Bae YH. Doxorubicin loaded pH-sensitive polymeric micelles for reversal of resistant MCF-7 tumor. *J Control Release*. 2005;103:405–418.
31. Na K, Lee ES, Bae YH. Adriamycin loaded pullulanacetate/sulfonamide conjugate nanoparticles responding to tumor pH: pH-dependent cell interaction, internalization and cytotoxicity in vitro. *J Control Release*. 2003;87:3–13.
32. Na K, Lee KH, Bae YH. pH-sensitivity and pH-dependent interior structural change of self-assembled hydrogel nanoparticles of pullulan acetate/oligo-sulfonamide conjugate. *J Control Release*. 2004;97:513–525.
33. Benns JM, Choi JS, Mahato RI, Park JS, Kim SW. pH-sensitive cationic polymer gene delivery vehicle: N-Ac-poly(L-histidine) polyHis-graft-poly(L-lysine) comb shaped polymer. *Bioconjug Chem*. 2000;11:637–645.
34. Liu R, Li D, He B, et al. Anti-tumor drug delivery of pH-sensitive poly(ethylene glycol)-poly(L-histidine)-poly(L-lactide) nanoparticles. *J Control Release*. 2011;152:49–56.
35. Kim D, Lee ES, Park K, Kwon IC, Bae YH. Doxorubicin loaded pH-sensitive micelle: antitumoral efficacy against ovarian A2780/DOX tumor. *Pharm Res*. 2008;25:2074–2082.
36. Gao J, Ming J, He B, Fan Y, Gu Z, Zhang X. Preparation and characterization of novel polymeric micelles for 9-nitro-20-(S)-camptothecin delivery. *Eur J Pharm Sci*. 2008;34:85–93.

Supporting information

Synthesis of α-methoxy-ω-amino-poly(ethylene glycol) (mPEG-NH_2)

mPEG (5 g, 2.5 mmol) was dissolved in anhydrous dichloromethane (75 mL) and the solution was cooled in an ice bath. Subsequently, triethylamine (1.8 mL, 12.5 mmol) and mesyl chloride (0.97 mL, 12.5 mmol) were added dropwise under stirring. The mixture was warmed to room temperature and stirred overnight in a nitrogen atmosphere. The mixture was filtrated, concentrated in vacuum, and precipitated in excess cold diethyl ether. The product was recrystallized in ethanol, collected and dried in vacuum overnight. The purified mPEGmesylate was added to 100 mL of a 25 wt% ammonia water solution. The mixture was vigorously stirred for 3 days at room temperature. The solution was extracted for four times with dichloromethane. The extract was dried with anhydrous magnesium sulfate and filtrated. The solvent was removed by rotatory evaporator. The crude product was purified by recrysallization in ethanol twice. The purified product was collected and dried in vacuum (yield = 60%).[1,2]

Purification of N^{α}-CBZ-N^{im}-DNP-L-histidine

N^{α}-CBZ-N^{im}-DNP-L-histidine was purified by recrysallization in acetic ester–petroleum ether (2:1, v/v) at 78°C. The purified N^{α}-CBZ-N^{im}-DNP-L-histidine was dried over phosphorus pentoxide in vacuum.

Synthesis of N^{im}-DNP-L-histidine carboxyanhydride (HisNCA)

The purified N^{α}-CBZ-N^{im}-DNP-L-histidine (4.4 mmol) was dissolved in anhydrous THF (30 mL) and 3 equivalents thionyl chloride was added. The solution changed from

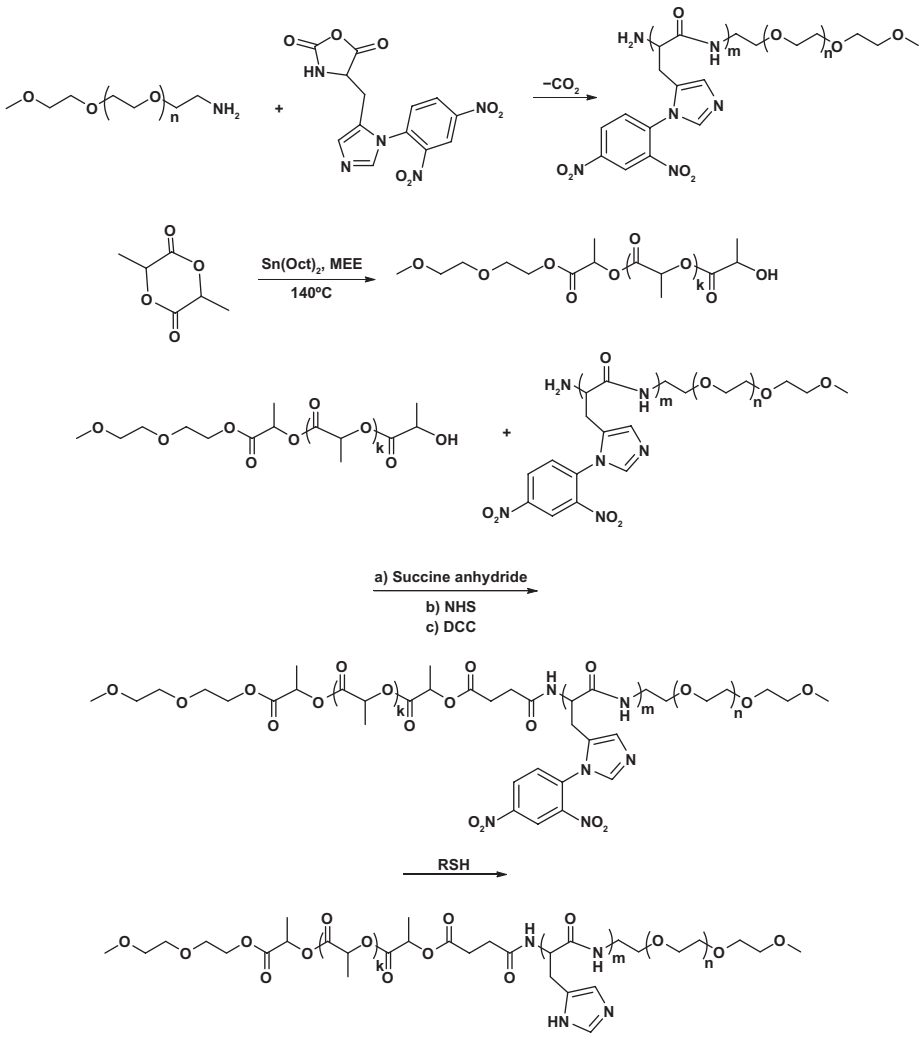

Figure S1 The synthetic route of mPEG-PH-PLLA triblock copolymer.
Abbreviations: NHS, N-Hydroxysuccinimide; DCC, N,N'-Dicyclohexylcarbodiimide; MEE, methoxyethoxyethanol.

opaque to transparency after a few minutes. The reaction was kept under nitrogen atmosphere at 25°C for 1 hour. The N^{im}-DNP-L-histidine carboxyanhydride hydrochloride was obtained after precipitation from excess diethyl ether. The further purification was according to the process described before[3] (yield = 33%).

Synthesis of protected mPEG-PH

The protected mPEG-PH diblock copolymer was prepared by ring-opening polymerization. Prescribed amount of $mPEG_{45}$-NH_2 and N^{im}-DNP-L-histidine carboxyanhydride was put into a flask with purified anhydrous DMF under a nitrogen atmosphere. The polymerization was carried out at 25°C for 72 h. The diblock copolymer was purified by precipitation in excess cold diethyl ether. To remove the impurities, the product was dissolved in 1 mL DMSO. Subsequently it was added dropwise into 25 mL deionized water. The solution was stirred for 15 minutes and then transferred into a dialysis membrane tube (MWCO 2000) and dialyzed against deionized water for 12 h. The outer phase was replaced with fresh deionized water at an interval of 4 hours. The solution inside the membrane was freeze-dried. The diblock copolymer was stored in vacuum (yield = 15%).

Synthesis of poly(L-lactide)

L-lactide monomer was purified by recrystallization in dry toluene. The monomer was dried in vacuum. The poly(L-lactide) sample was synthesized by ring-opening polymerization of L-lactide using stannous octoate as catalyst and methoxyethoxyethanol as initiator under vacuum at 140°C for 48 h. The resulted polymer was purified by precipitation, using chloroform as the solvent and cold methanol as the precipitant[4] (yield = 90%).

Synthesis of monocarboxylated poly (L-lactide)

Monocarboxylated poly(L-lactide) was prepared by reacting poly(L-lactide) with 5 equivalents succinic anhydride in the presence of DMAP as the catalyst. The reaction was stirred in purified anhydrous chloroform at 30°C for 72 h. Thereafter, the product was precipitated with cold methanol and dried under vacuum (yield = 85%).

Activation of monocarboxylated poly (L-lactide) (PLLA-NHS)

The monocarboxylated poly(L- lactide) was activated using NHS and DCC in DCM for 24 h. The solution was filtered to remove the dicyclohexylurea (DCU) and then diethyl ether was added to precipitate the activated monocarboxylated poly(L-lactide) (yield = 85%).

Synthesis of protected mPEG-PH-PLLA

The protected mPEG-PH-PLLA was prepared by coupling reaction. PLLA-NHS was reacted with 1 equivalent PEG-PH in DMF-DCM (2:1, v/v) in the presence of DCC for 72 h. This solution was filtered to remove insoluble moieties, and then the solvent was removed by rotatory evaporator. Thereafter, the original product was dissolved in DCM. The insoluble moieties were removed by filtration. The product was precipitated in cold diethyl ether and then dried in vacuum for 2 days (yield = 15%).

Deprotection of mPEG-PH-PLLA

The protected mPEG-PH-PLLA and 2-mercaptoethanol were dissolved and stirred in DMF at 30°C for 24 h. The product was precipitated with cold diethyl ether. The precipitate was then dialyzed against deionized water using a dialysis membrane tube (MWCO 2000). After 24 h dialysis, the product was freeze-dried (yield = 30%).

Figure S2 showed the ^{1}H NMR spectra of mPEG-NH_2, mPEG-PH diblock copolymer and mPEG-PH-PLLA triblock copolymer. In the spectrum of mPEG-NH_2, the chemical shift of the protons of CH_2CH_2O (2) appeared at δ = 3.68 ppm. The chemical shift of protons in the terminal CH_3 (1) groups was at δ = 3.38 ppm. The other two signal peaks appeared at δ = 3.53 and 2.88 ppm were attributed to the protons of $OCH_2CH_2NH_2$ (3) and $OCH_2CH_2NH_2$ (4), respectively. The protons in NH_2 (5) were active and located at δ = 1.71 ppm.

In the spectrum of protected mPEG-PH diblock copolymer, the chemical shifts of the protons were complicated. Because of the solvent change, the proton signals of CH_2CH_2O in mPEG block were shifted to δ = 3.50 ppm. The signals of protons 1 and 3 were gathered together with proton 2. The peak of proton 4 was shifted in the range from δ = 3.15 to 3.25 ppm because of the chemical environment variation after the ring-opening polymerization. The proton signals of the CH (6) in PH backbones and CH_2 (7) in pendant groups appeared at δ = 4.24 and 3.15 ppm. The signal of proton 7 split into multi-peaks and overlapped the signal of proton 4. Because of the conjugation, all the protons in the pendant groups appeared in low magnetic field area. The signals of the protons (8 and 9) in imidazole groups were split multi-peaks and the chemical shifts were δ = 7.52 and 8.02 ppm. There were three protons (10, 11 and 12) in the protected 2, 4-dinitrophenyl group. The chemical shifts of the three

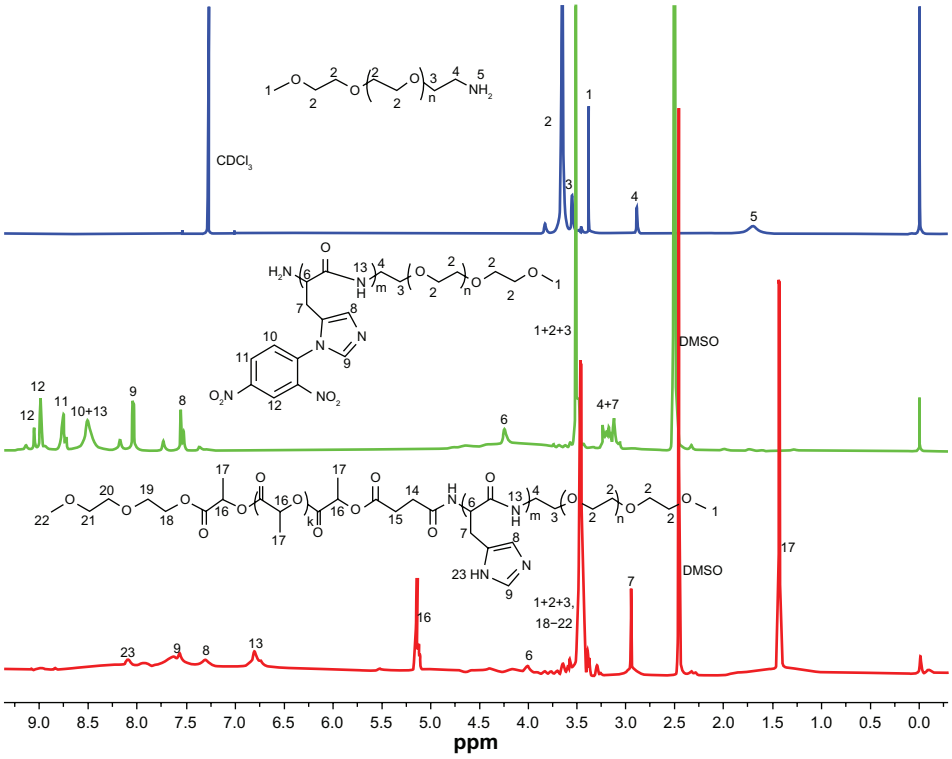

Figure S2 The ^{1}H NMR spectra of mPEG$_{45}$-NH$_2$, mPEG$_{45}$-PH$_{30}$ and mPEG$_{45}$-PH$_{30}$-PLLA$_{82}$.
Abbreviation: ppm, parts per million.

protons were δ = 8.50, 8.74 and 8.99 ppm, respectively. The proton of 12 in 2, 4-dinitrophenyl group also split into multi-peaks for its complicated chemical environment. The proton of NH in the PH backbones was shifted to δ = 8.50 ppm and it overlapped the signal of proton 13 in protected 2, 4-dinitrophenyl group. The ratio of the integrity between CH (6) in PH backbone and CH_2CH_2O (2) in mPEG blocks was used to calculated the number of repeated units of L-histidine in the mPEG-PH diblock copolymers.

The chemical shifts of the protons in PH blocks changed greatly after the deprotection. Two new strong peaks appeared at δ = 1.42 and 5.13 ppm, which were assigned to the protons of CH_3 (17) and CH (16) in PLLA blocks. The little shift of the protons in mPEG blocks was from 3.50 to 3.48 ppm. As methoxyethoxyethanol was used as initiator to control the chain length of PLLA blocks, the chemical shifts of the protons in methoxyethoxyethanol were located around the main peak of mPEG blocks for the similar chemical environment. All the chemical shifts of the protons in PH blocks shifted to higher magnetic field and the shape of the peaks was changed greatly. The peaks of proton 8 and 9 in pendant imidazole groups became wide and weak. They appeared at δ = 7.28 and 7.57 ppm. A new peak of NH (23) in deprotected imidazole groups appeared at δ = 8.08 ppm. As active hydrogen, the proton of NH (13) in PH backbone shifted to δ = 6.77 ppm. The chemical shifts of proton 6 and 7 in deprotected tri-block copolymers were shifted to δ = 4.00 and 2.97 ppm, respectively. All the intensity of the proton peaks in PH blocks in the deprotected triblock copolymer were lower than those in protected mPEG-PH diblock copolymers because it was hard to find a proper solvent for all the three blocks. For example, d_6-DMSO was good for mPEG and PLLA blocks but not ideal for deprotected PH blocks.

The ratio of the intensity between OCH_2CH_2 (2) in mPEG segments and CH (6) in PH was used to calculate the repeated units of L-histidine in PH segments. The molecular weight

Table S1 Characterizations of mPEG-PH-PLLA triblock copolymer nanoparticles

Sample	Received[a]	Designed[b]	Mn[c]	DLC (%)	EE (%)
1	mPEG$_{45}$-PH$_{15}$-PLLA$_{82}$	mPEG$_{45}$-PH$_{17}$-PLLA$_{82}$	10388	9.6	24.5
2	mPEG$_{45}$-PH$_{30}$-PLLA$_{82}$	mPEG$_{45}$-PH$_{39}$-PLLA$_{82}$	12668	13.2	27.7

Notes: [a]The repeated units of L-histidine in the copolymers were calculated from ^{1}H NMR spectra of mPEG-PH diblock copolymers; [b]the designed feeding dose; [c]calculated from ^{1}H NMR spectra of mPEG-PH-PLLA tiblock copolymers.
Abbreviations: DLC, drug loading content; EE, encapsulation efficiency; Mn, number average molecular weight.

of PLLA segment was regulated by the molar ratio between monomer L-lactide and initiator methoxyethoxyethanol. The molecular weight of the copolymers calculated from ^{1}H NMR spectra was presented in Table S1.

References

1. Zalipsky S. Functionalized poly(ethy1ene glycol) for preparation of biologically relevant conjugates. *Bioconjugate Chem*. 1995;6:150–165.
2. Aronov O, Horowitz AT, Gabizon A, Gibson D. Folate-targeted PEG as a potential carrier for carboplatin analogs. Synthesis and in vitro studies. *Bioconjugate Chem*. 2003;14:563–574.
3. Lee ES, Shin HJ, Na K, Bae YH. Poly(L-histidine)-PEG block copolymer micelles and pH-induced destabilization. *J Controlled Release*. 2003;90:363–374.
4. Deng XM, Xiong CD, Cheng LM, Xu RP. Synthesis and characterization of block copolymers from D, L-lactide and poly(ethylene glycol) with stannous chloride. *J Polym Sci, Part C: Polym Lett*. 1990;28:411–416.